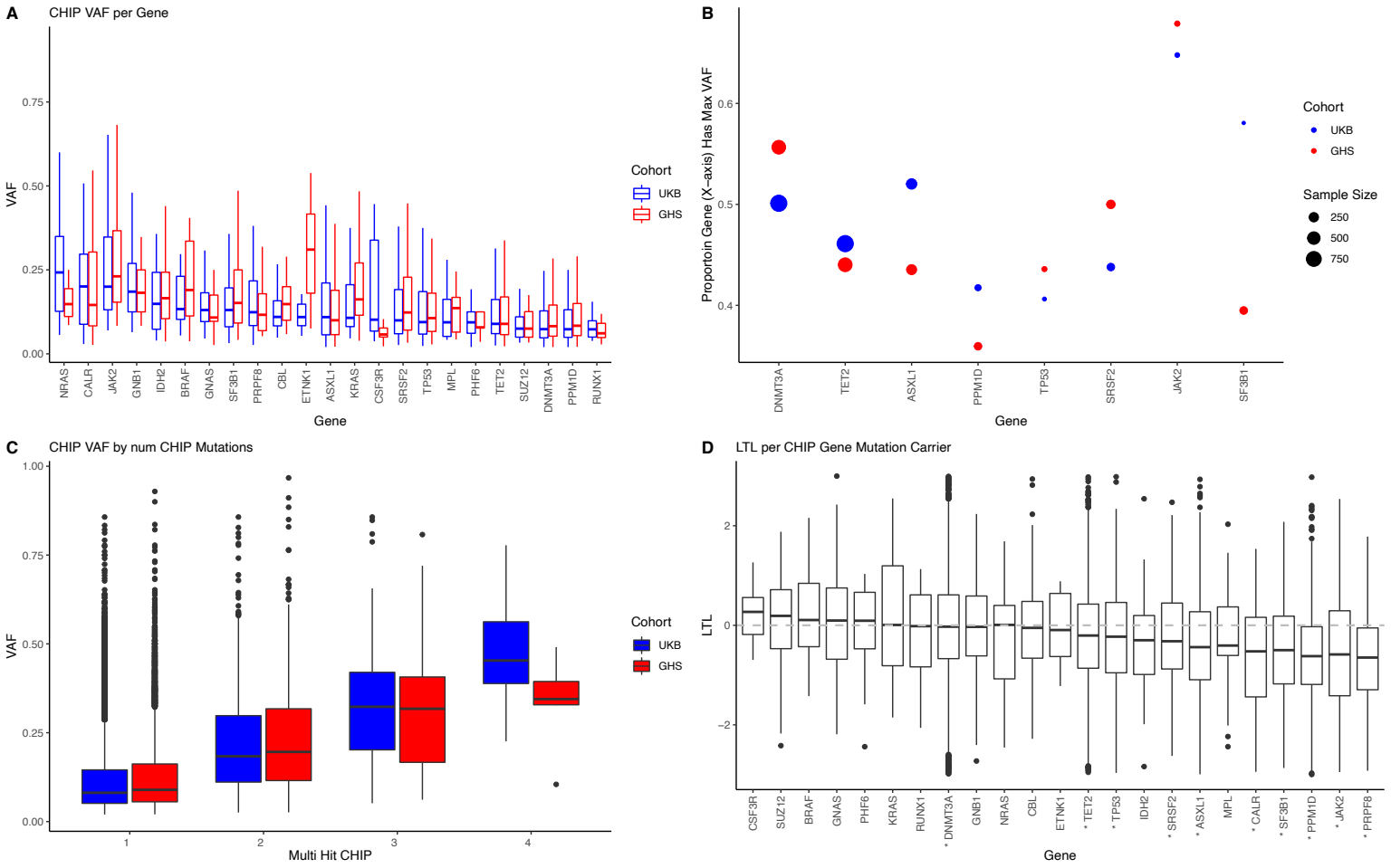


**Figure S1: Variant Allele Fraction (VAF) and Leukocyte Telomere Length (LTL) Distributions by Specific CHIP Gene Carrier Status. A.** Distributions of variant allele fraction (VAF, y axis) are shown for mutations within each of the 23 CHIP genes in our callset across individuals with only a single CHIP mutation from UKB (blue) and GHS (red). Canonical CHIP genes generally had low VAFs compared with mutations more canonically associated with leukemias. **B.** Among individuals with multiple CHIP mutations (i.e. $\geq 2$) where at least 1 was in the gene on the x-axis, the proportion of times the CHIP mutation in the x-axis gene was the one with the highest VAF is shown (y axis) for the top 8 CHIP genes. Higher proportions suggest that those CHIP genes represent either the driver mutation for CHIP or presence in the largest CHIP clone. **C.** The maximum VAF among all CHIP mutations is higher in individuals with increasing numbers of CHIP mutations. D. Distributions of telomere length (LTL) are shown across 23 CHIP gene mutation carriers in our callset. The asterisk (*) in front of the x-axis gene label denotes that carriers of CHIP mutations in that gene had LTL lengths that differed significantly from zero (two-sided Wilcoxon Rank-Sum test, $P \leq 0.0022$, i.e. 0.05/23). Box and whisker plots show median values at the centre, 75$^{th}$ and 25$^{th}$ percentiles at the box boundaries, feature whiskers that represent up to 1.5 times the interquartile range (IQR) beyond the box boundaries, and dots for any points greater or less than these whisker boundaries.

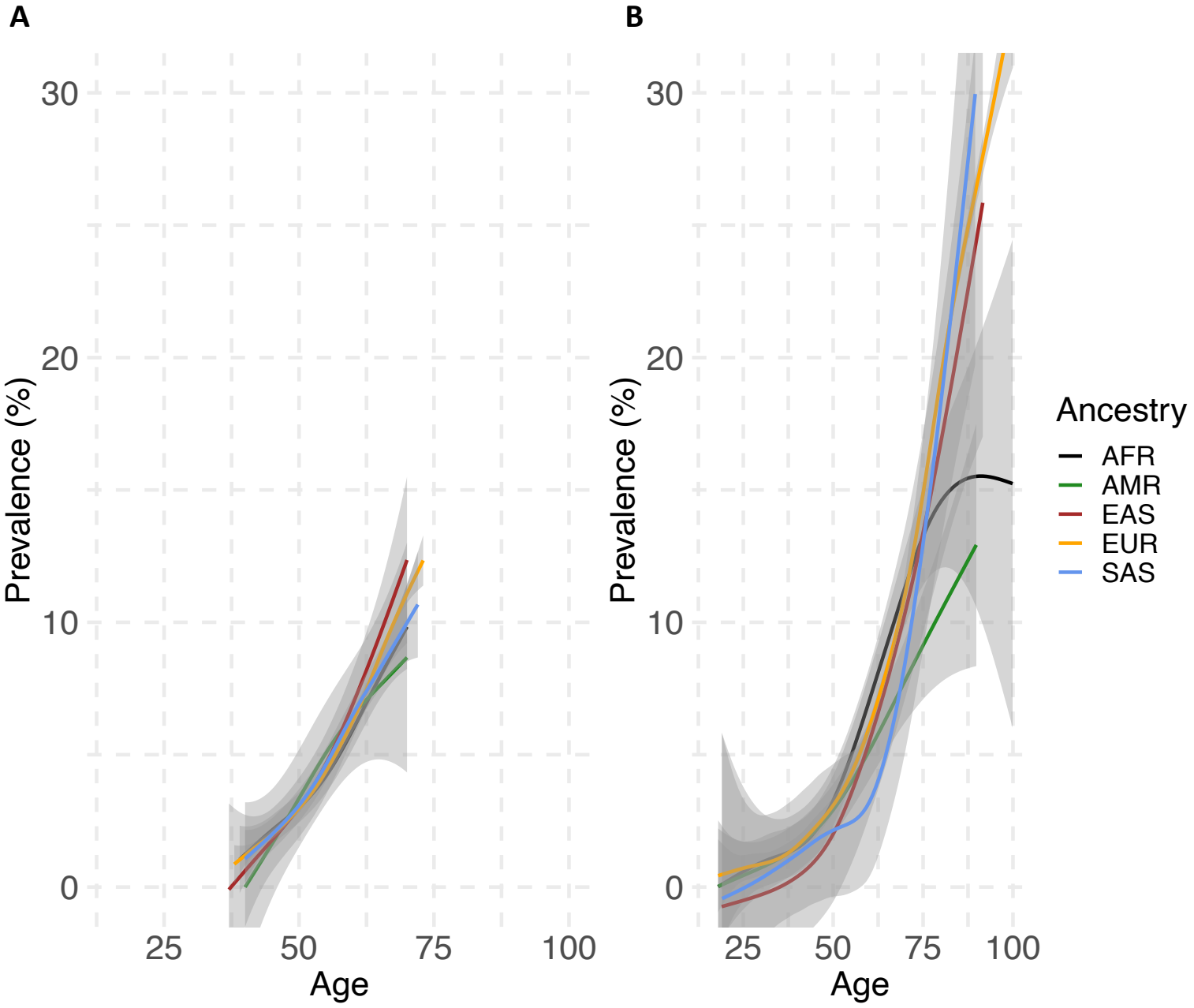


**Figure S2: CHIP prevalence across ancestries. A-B.** Splines showing the prevalence of CHIP mutations by age across different continental ancestries in the UKB **(A)** and GHS **(B)** cohorts. Centre lines represent the general additive model spline and the shaded regions represent 95% confidence intervals.

**A**

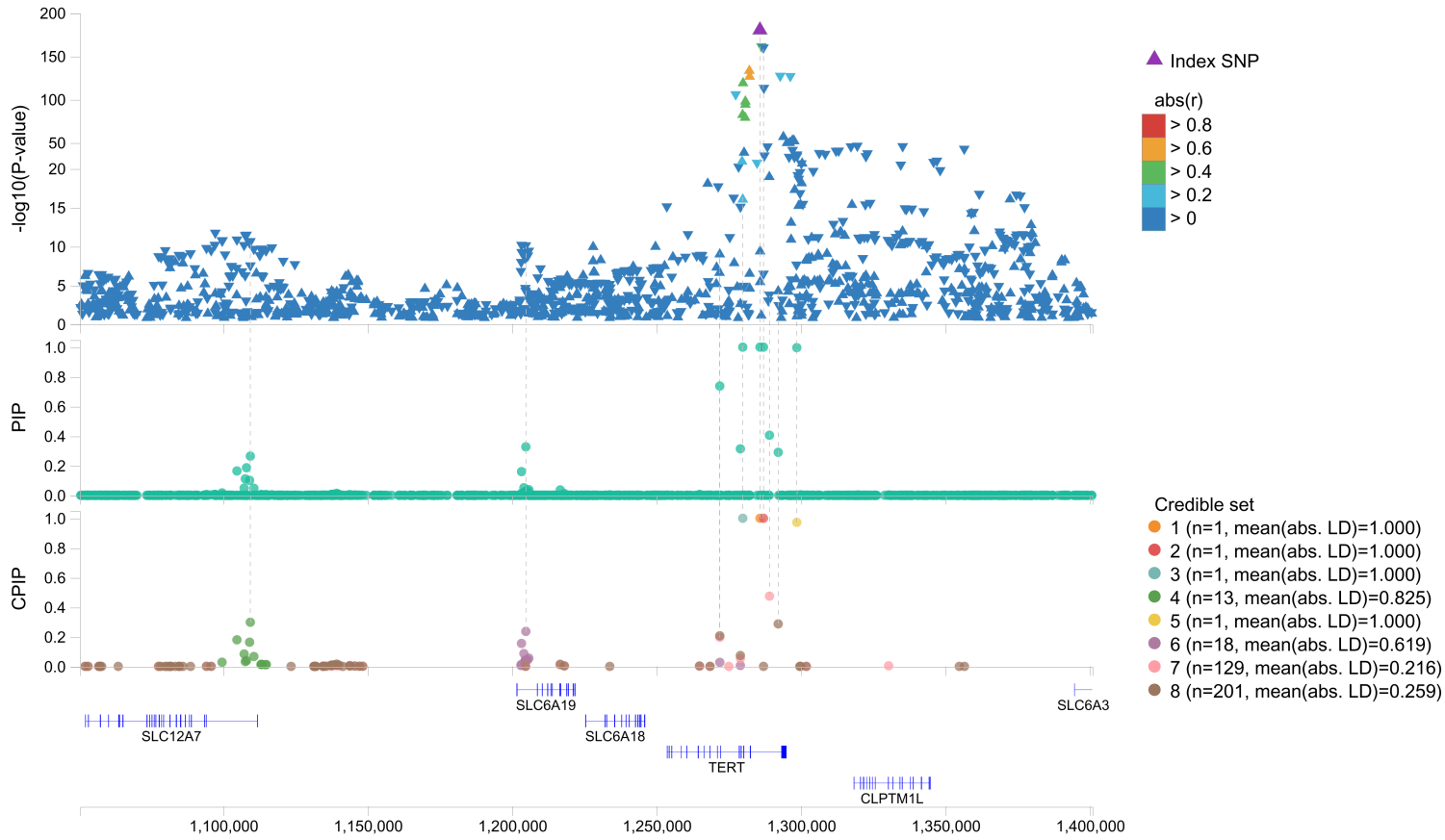


**B**

| Variant | C&T | COJO | Finemap (CS, Prob, Lead) |
|---|---|---|---|
| 5:1285859:C:A | Yes | Yes | Yes (1, 1, Yes) |
| 5:1287079:G:A | No | Yes | Yes (2, 1, Yes) |
| 5:1279913:G:A | No | No | Yes (3, 1, Yes) |
| 5:1109453:T:C | No | No | Yes (4, 0.30, Yes) |
| 5:1298618:A:C | No | Yes | Yes (5, 0.97, Yes) |
| 5:1204825:C:T | No | No | Yes (6, 0.24, Yes) |
| 5:1289162:G:A | No | No | Yes (7, 0.47, Yes) |
| 5:1292184:G:A | No | No | Yes (8, 0.29, Yes) |
| 5:720334:A:G | No | Yes | Yes (8, 0.05, No) |
| 5:1109199:G:C | No | Yes | Yes (4, 0.16, No) |

**Figure S3: Finemapping results at the *TERT* locus on chromosome 5. A.** Association results results across the *TERT* locus are shown, including finemaping results that highlight variant inclusion probabilities across 8 credible sets. P-values are uncorrected and derive from two-sided tests performed using approximate Firth logistic regression and subsequent meta analysis **B.** SNPs priorities by COJO or FINEMAP are highlighted. PIP: Posterior Inclusions Probability, CPIP: Conditional Posterior Inclusion Probability.

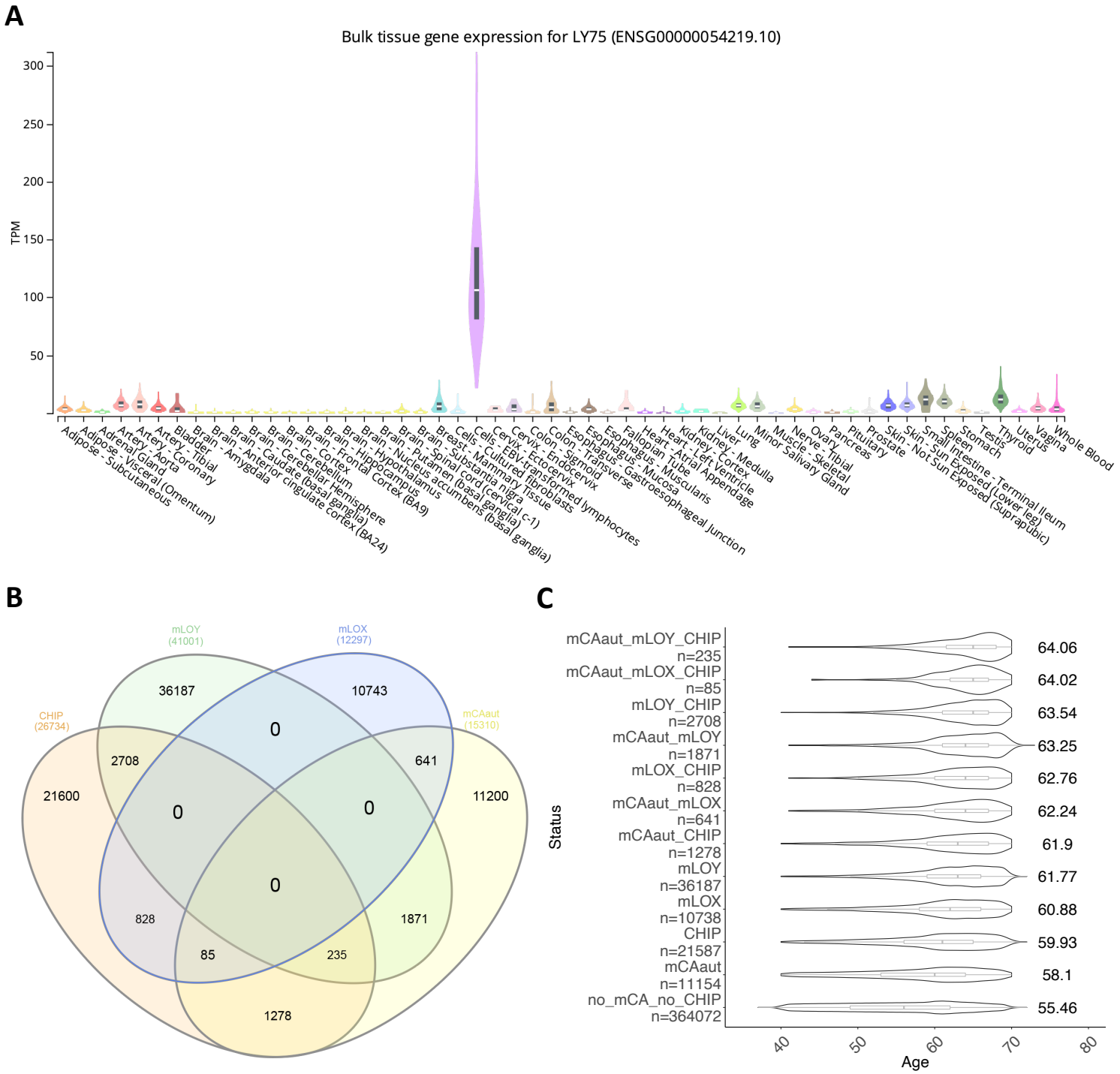


**Figure S4. Overlap of CHIP and mCA phenotypes and average ages across CH carriers. A.** Bulk Tissue gene expression from GTEx for *LY75* show lymphocyte specific expression. Boxplot centre points represent the median expression values, with boxes bounded by the 75$^{th}$ and 25$^{th}$ percentiles. **B.** Venn diagram showing the overlap between CHIP and other somatic mosaic alteration phenotypes across samples from UKB **C.** Violin plots of the age distributions of carriers of CHIP and/or mCA phenotypes are shown (label = distributional mean), along with box and whisker plots that show median values at the center, 75$^{th}$ and 25$^{th}$ percentiles at the box boundaries, and whiskers representing up to 1.5 times the interquartile range (IQR). Individuals without any CHIP or mCA are the youngest, and individuals with an increasing number of somatic lesions are older on average.

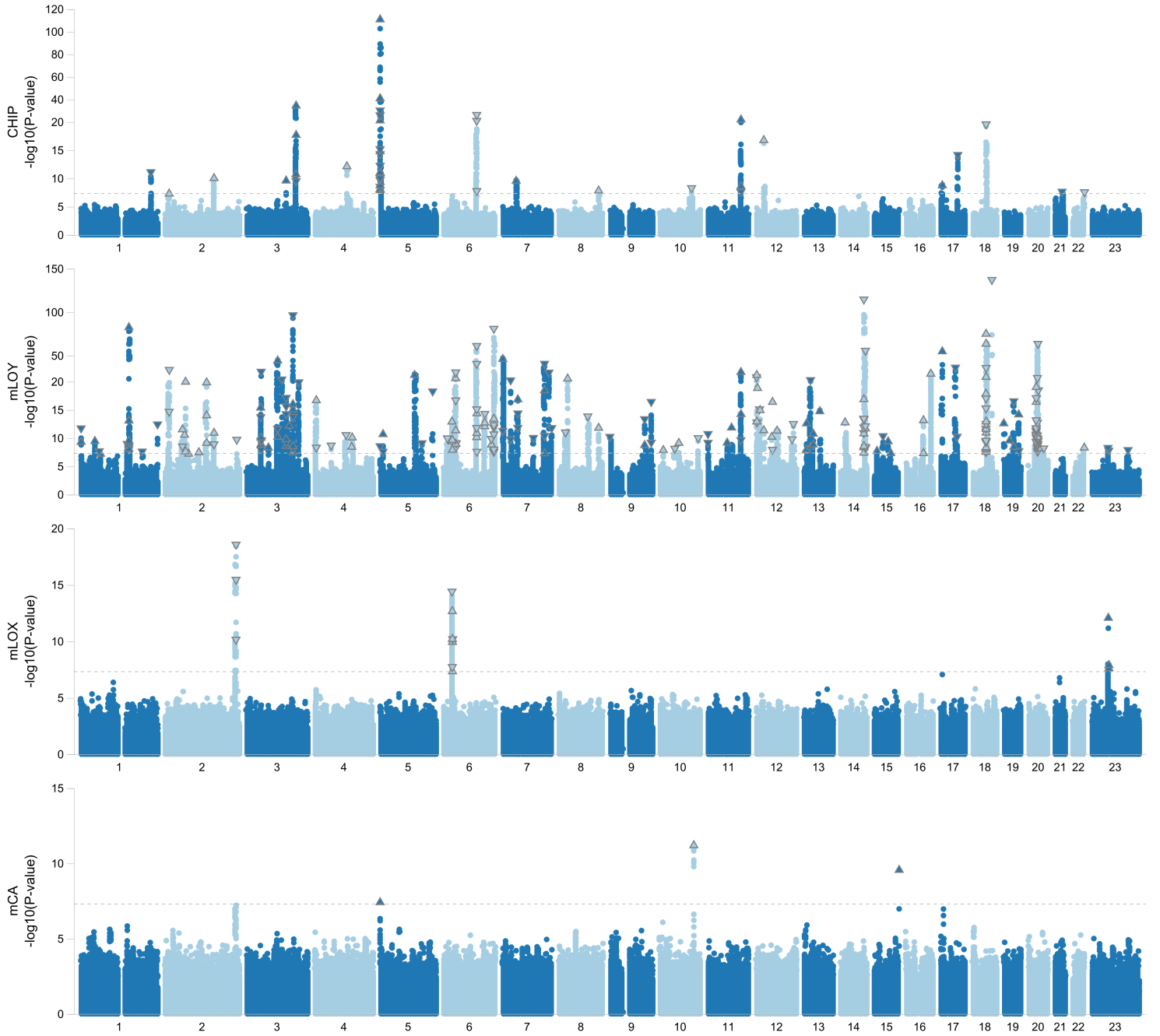


**Figure S5. Manhattan plots from GWAS of CHIP and mCA phenotypes.** Manhattan plots of results from association analyses of exclusive CHIP and mCA phenotypes (i.e. carriers have only CHIP or only mosaic chromosomal alterations). The majority of significantly associated loci are found in association with CHIP and/or mLOY. Association models were run with age, age$^2$, sex, and age-by-sex, and 10 ancestry-informative principal components (PCs) as covariates.

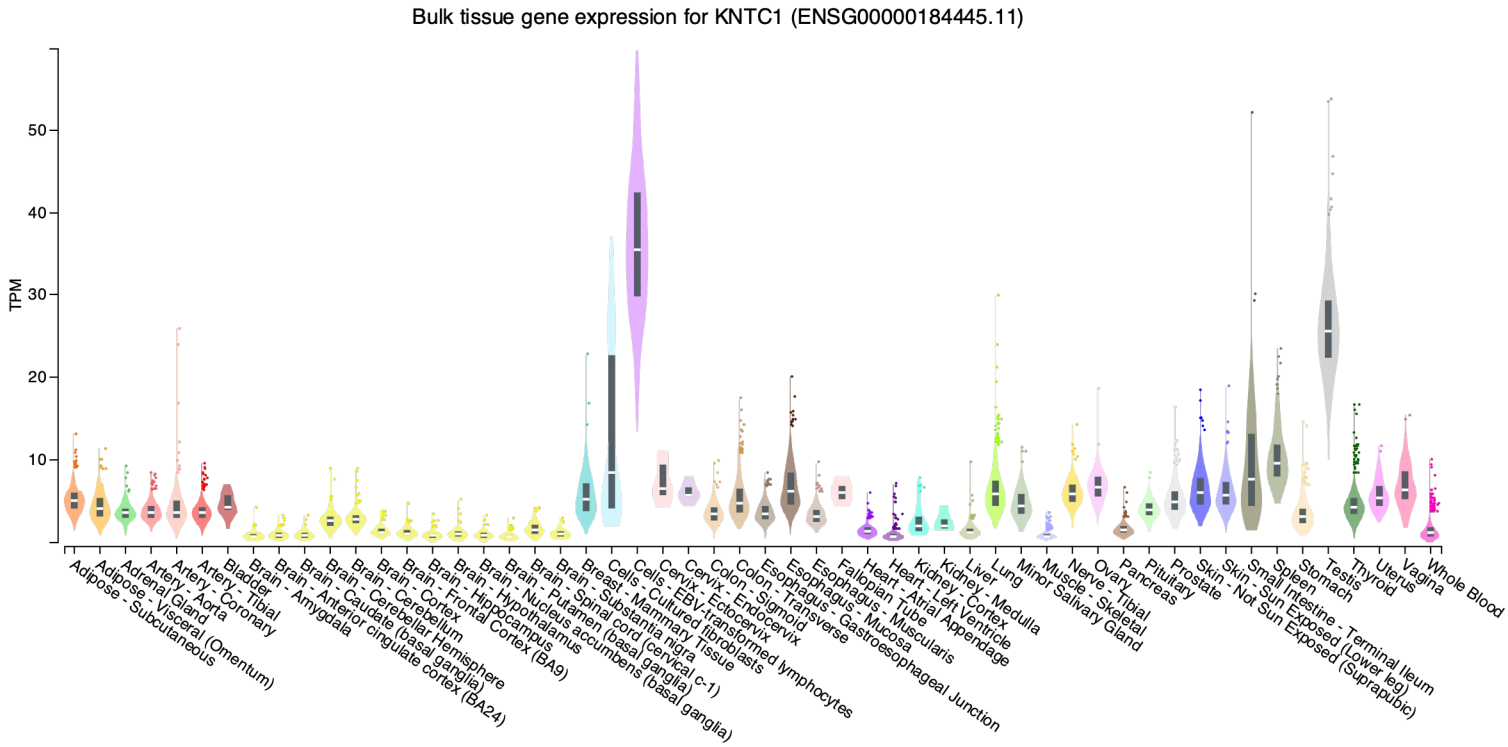


**Figure S6: KNTC1 expression across tissue type.** Barplots of expression level (transcript per million, y axis) for the *KNTC1* gene across tissues, as ascertained by Genotype-Tissue Expression (GTEx) project via bulk RNA Sequencing. Boxplot centre points represent the median expression values, with boxes bounded by the 75$^{th}$ and 25$^{th}$ percentiles.


## Figure S7. Comparison of Associations Across Phenotypes Associated with CHIP

Association results are visualized across all traits (y-axis) that are associated (P <= 1e-5) with at least one CHIP gene subtype (y-axis). Dot color represents effect size direction, and dot size is scaled to the log10 value of the effect size. Background color represents trait category, and is the same as in Figure 5, although the alpha value is reduced so that the effect size dots can be readily seen. Association models were run with age, age$^2$, sex, and age-by-sex, and 10 ancestry-informative principal components (PCs) as covariates.

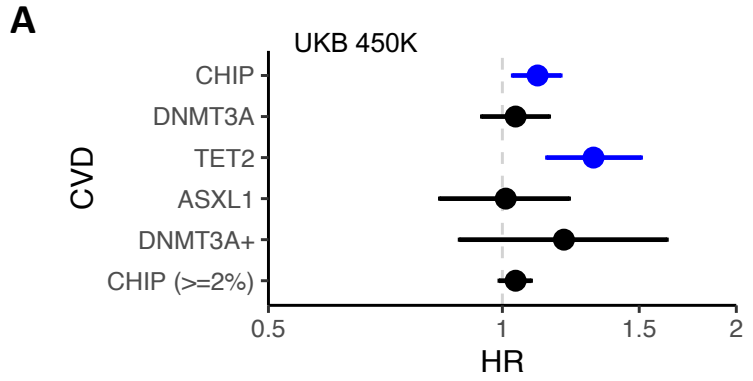


| Total | Event | HR(LCI, UCI) | P-value |
|---|---|---|---|
| 8165 | 783 | 1.11 (1.03, 1.19) | 4.2e−03 |
| 4767 | 396 | 1.04 (0.94, 1.15) | 0.47 |
| 1739 | 199 | 1.31 (1.14, 1.51) | 1.3e−04 |
| 878 | 105 | 1.01 (0.83, 1.22) | 0.95 |
| 360 | 40 | 1.2 (0.88, 1.63) | 0.26 |
| 19682 | 1709 | 1.04 (0.99, 1.09) | 0.12 |

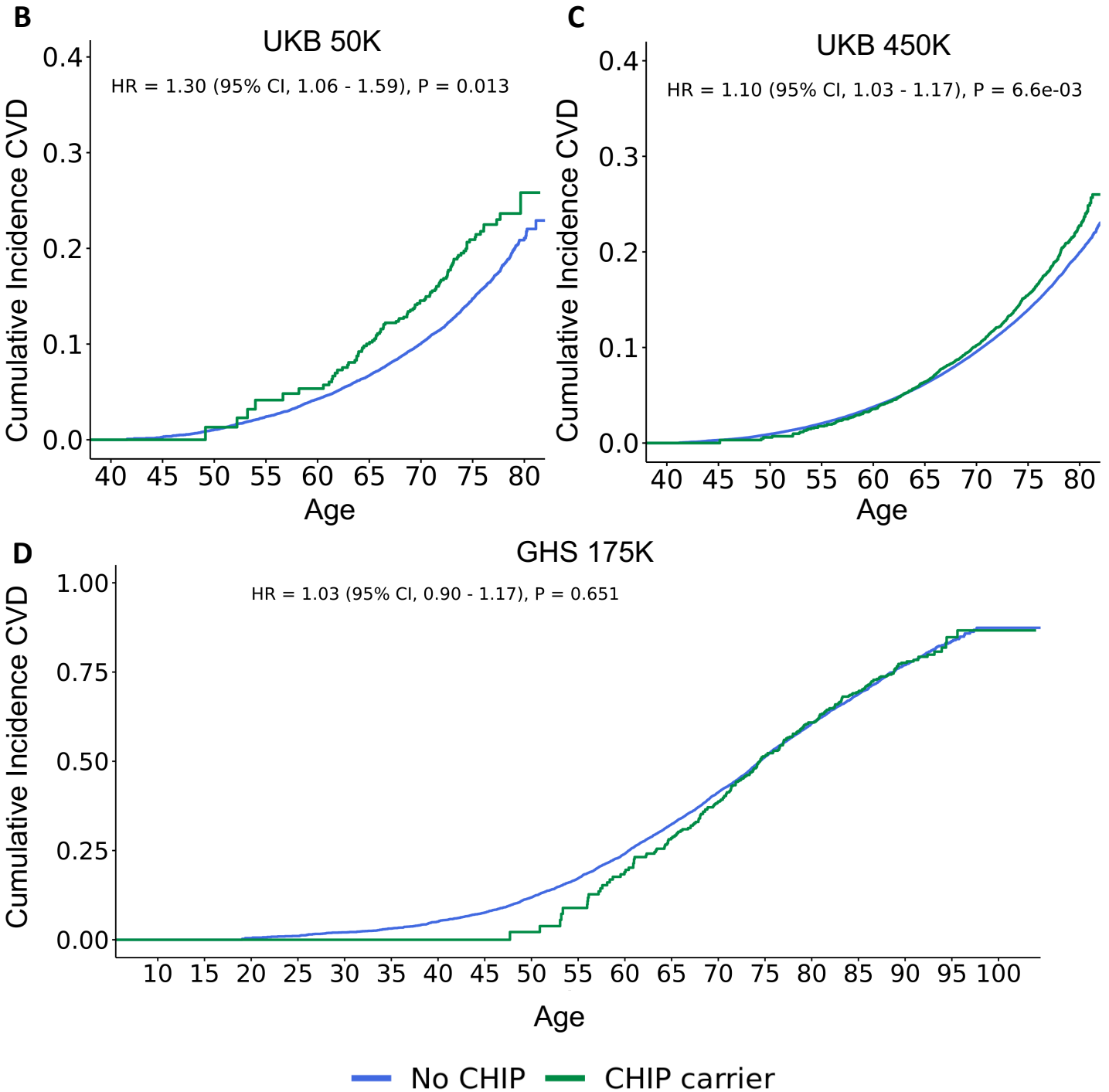


**Figure S8: CVD Incidence among CHIP carriers in UKB 50K vs UKB 450K. A.** Breaking down CVD risk among CHIP carriers from the UKB cohort according to CHIP gene mutation suggests that risk is driven by *TET2* mutations (OR = 1.31, P = $1.80 * 10^{-4}$). **B-C.** Survival curves are drawn showing the increased risk of CVD for CHIP carriers (green), compared to individuals without CHIP (blue), across the UKB cohort. In the first 50,000 individuals from UKB **(B),** this risk is higher (OR = 1.30) than in the full cohort **(C,** OR = 1.10). **D.** No increased risk of CVD is found among CHIP carriers (green) from the GHS cohort compared to individuals without CHIP (blue). Models are adjusted for sex, LDL, HDL, pack years, smoking status, BMI, essential primary hypertension, type 2 diabetes mellitus, and 10 European specific genetic PCs. Hazard ratios (HR) were estimated using cox-proportional hazard modeling, with p-values uncorrected and derived from two-sided Wald tests.

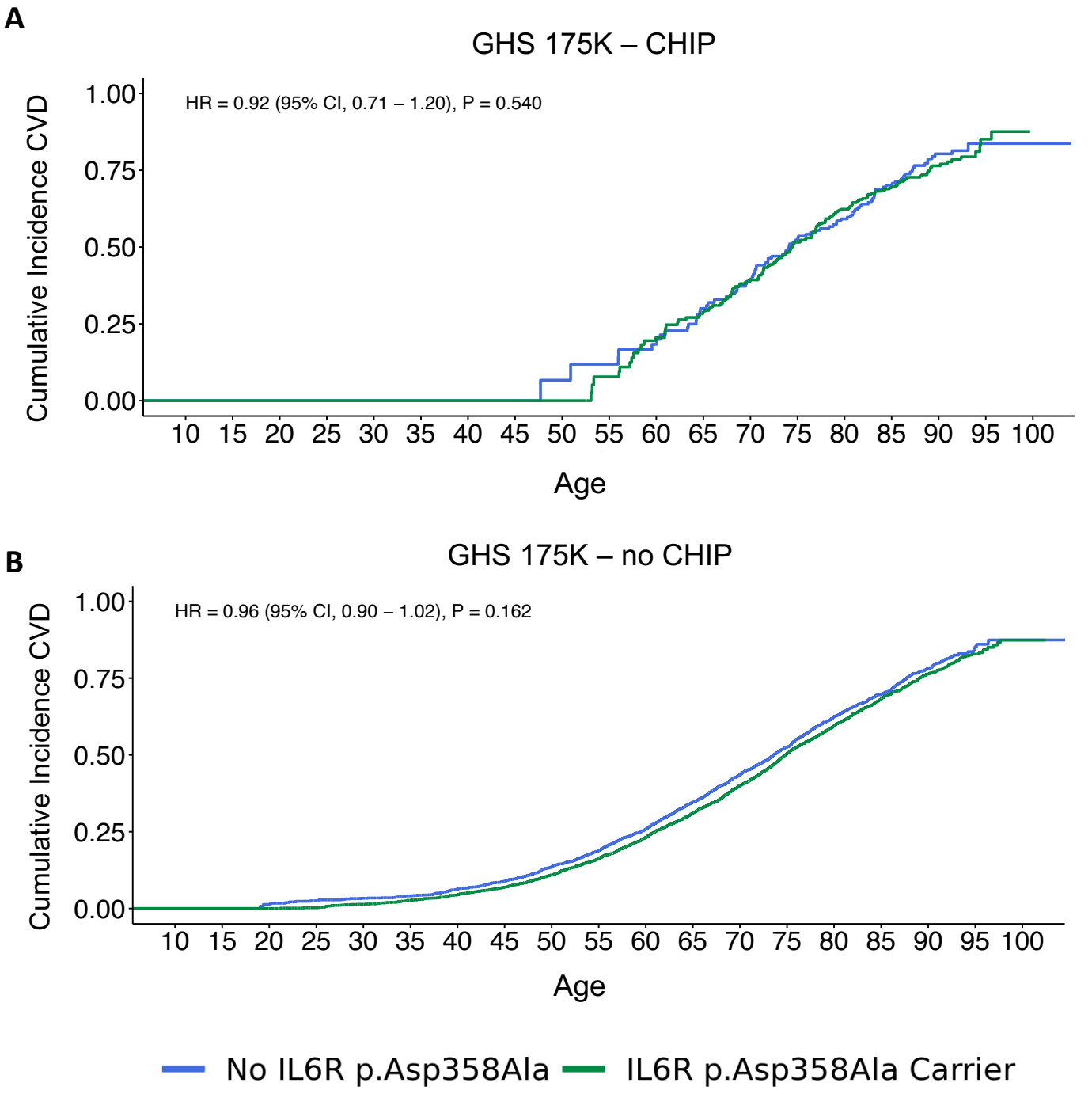


**Figure S9: CVD Incidence in IL6R Mutation Carriers with and without CHIP (GHS). A-B.** Survival curves are drawn showing that *IL6R* p.Asp358Ala mutation carriers (green) from GHS are not an elevated risk of CVD incidence (y-axis) compared with individuals without this mutation in individuals with **(A)** or without **(B)** CHIP. Models are adjusted for sex, LDL, HDL, pack years, smoking status, BMI, essential primary hypertension, type 2 diabetes mellitus, and 10 European specific genetic PCs. Hazard ratios (HR) were estimated using cox-proportional hazard modeling, with p-values uncorrected and derived from two-sided Wald tests.

**A**

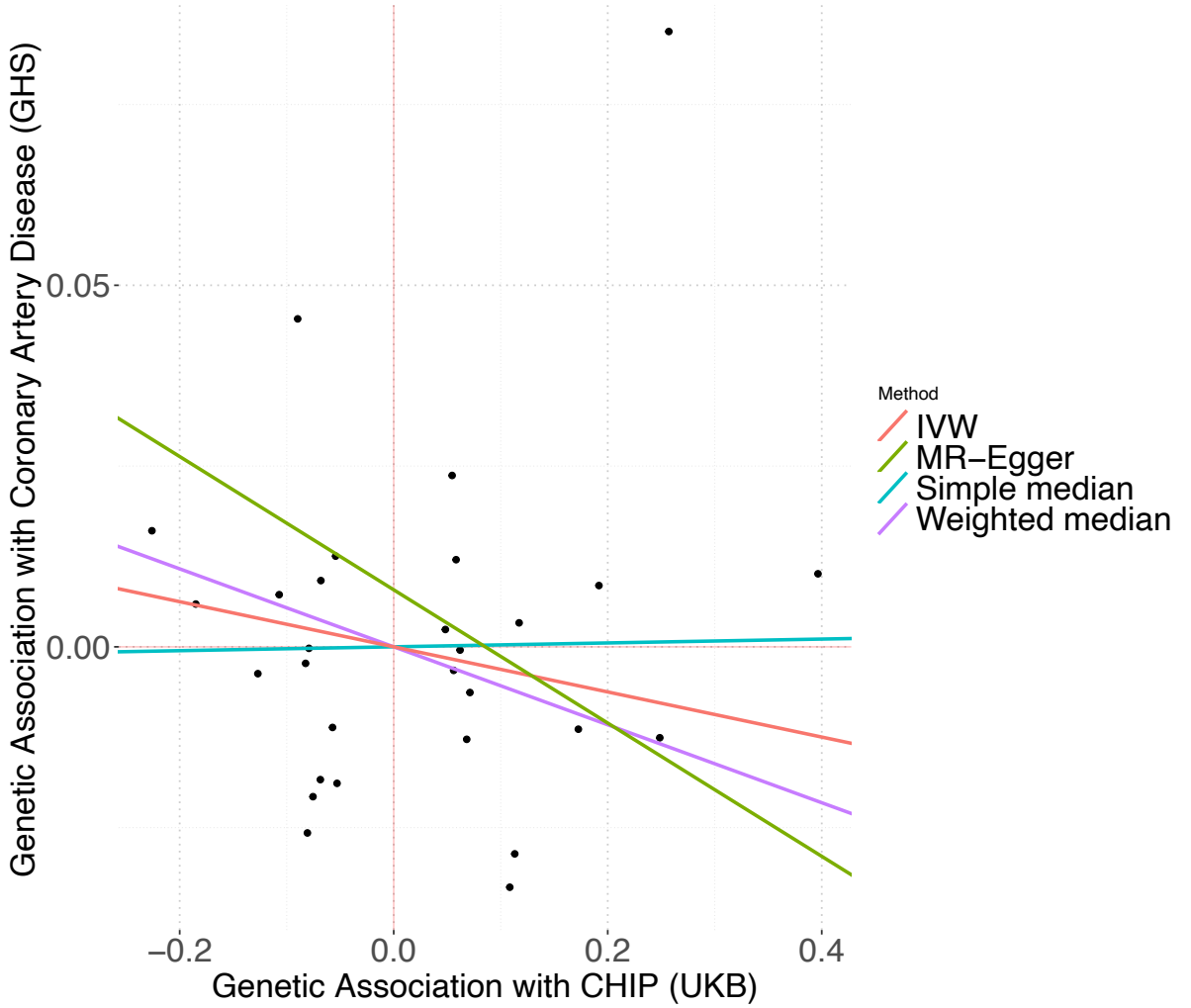


**B**

| **Exposure: CHIP (UKB) \| Outcome: Coronary Artery Disease (GHS)** | | | MR without *TERT* variants | |
|---|---|---|---|---|
| **Method** | **OR (95% CI)** | **P value** | **OR** | **P value** |
| Simple median | 1.00 (0.93-1.08) | 0.94 | 1.00 (0.92-1.09) | 0.95 |
| Weighted median | 0.95 (0.89-1.01) | 0.079 | 1.00 (0.92-1.09) | 0.94 |
| Penalized weighted median | 0.95 (0.89-1.01) | 0.081 | 1.03 (0.94-1.11) | 0.54 |
| IVW | 0.97 (0.92-1.02) | 0.26 | 0.99 (0.91-1.06) | 0.7 |
| Penalized robust IVW | 0.97 (0.93-1.01) | 0.2 | 1.00 (0.93-1.06) | 0.89 |
| MR-Egger | 0.91 (0.82-1.01) | 0.087 | 0.92 (0.76-1.12) | 0.41 |
| (intercept) | 1.01 (1.00-1.02) | 0.19 | 1.01 (0.99-1.02) | 0.47 |
| Penalized robust MR-Egger | 0.91 (0.86-0.97) | 0.0061 | 0.94 (0.79-1.11) | 0.45 |
| (intercept) | 1.01 (1.00-1.02) | 0.13 | 1.01 (0.99-1.02) | 0.51 |

**Figure S10: MR analysis of CHIP and CVD does not find a significant positive association between CHIP and CVD. A.** Plot showing estimated associations via four mendelian randomization (MR) methods between CHIP and CVD. Each point represents one of 29 instrumental variables (i.e. conditionally independent SNPs) that were identified in the UKB cohort as associated with CHIP. The x-axis shows the effect estimate (beta) of the SNP on CHIP in UKB, and the y-axis shows the effect estimate (beta) of the SNP on CVD in GHS. The slope of each regression line represents the effect size estimated by the respective MR methods. **B.** Statistical results are shown from seven MR methods with differing sensitivities to outliers and/or violations of the MR assumptions. The estimated intercept values are shown for the two MR-Egger-based methods that estimate these terms (yellow rows). No method provided support for a positive association between CHIP and CVD. Results from MR analyses run without variants at the *TERT* locus as instrumental variables are similarly feature no significant associations (B, grey text).

**A**

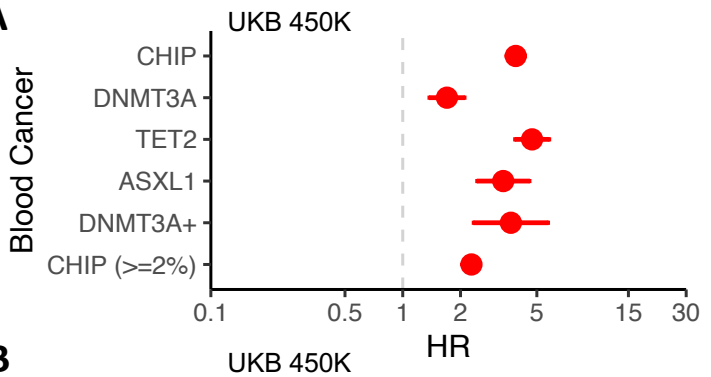


| Total | Event | HR(LCI, UCI) | P-value |
|---|---|---|---|
| 8826 | 520 | 3.88 (3.46, 4.36) | 9.1e−117 |
| 5091 | 148 | 1.7 (1.37, 2.11) | 1.5e−06 |
| 1880 | 144 | 4.72 (3.83, 5.83) | 1.7e−47 |
| 1015 | 76 | 3.34 (2.43, 4.6) | 1.3e−13 |
| 439 | 81 | 3.66 (2.33, 5.75) | 1.7e−08 |
| 21069 | 776 | 2.28 (2.08, 2.51) | 4.4e−67 |

**B**

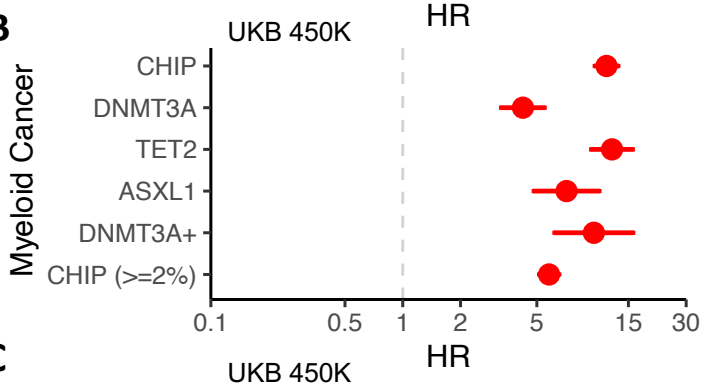


| Total | Event | HR(LCI, UCI) | P-value |
|---|---|---|---|
| 8797 | 399 | 11.53 (9.94, 13.38) | 1.3e−228 |
| 5085 | 98 | 4.23 (3.23, 5.53) | 7.3e−26 |
| 1877 | 100 | 12.32 (9.52, 15.93) | 1.5e−81 |
| 1012 | 57 | 7.14 (4.78, 10.67) | 9.3e−22 |
| 437 | 55 | 9.91 (6.13, 16.01) | 8.1e−21 |
| 21032 | 510 | 5.79 (5.1, 6.59) | 1.0e−158 |

**C**

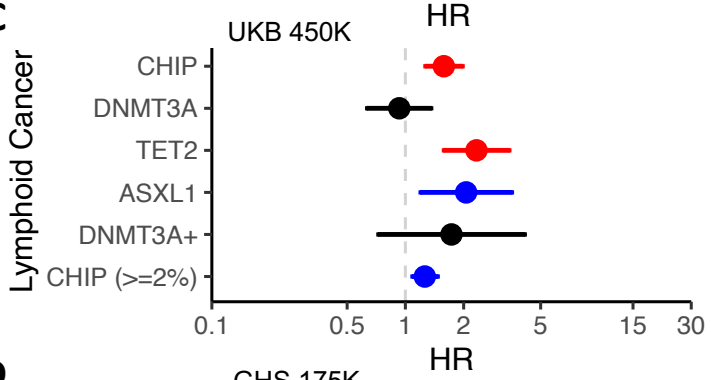


| Total | Event | HR(LCI, UCI) | P-value |
|---|---|---|---|
| 8891 | 127 | 1.58 (1.26, 1.99) | 9.3e−05 |
| 5099 | 49 | 0.93 (0.63, 1.37) | 0.71 |
| 1889 | 41 | 2.33 (1.57, 3.47) | 3.1e−05 |
| 1019 | 20 | 2.06 (1.19, 3.58) | 9.7e−03 |
| 445 | 28 | 1.73 (0.72, 4.17) | 0.22 |
| 21142 | 251 | 1.26 (1.08, 1.48) | 3.6e−03 |

**D**

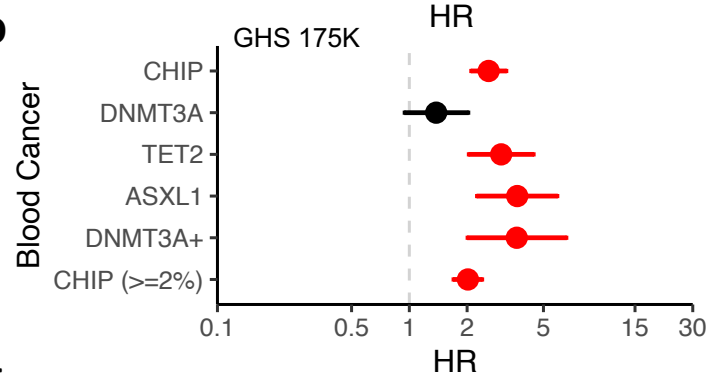


| Total | Event | HR(LCI, UCI) | P-value |
|---|---|---|---|
| 3003 | 101 | 2.59 (2.09, 3.22) | 8.1e−18 |
| 1541 | 27 | 1.38 (0.94, 2.04) | 0.1 |
| 673 | 27 | 3.01 (2.03, 4.47) | 4.1e−08 |
| 343 | 17 | 3.65 (2.24, 5.94) | 1.9e−07 |
| 195 | 11 | 3.63 (2, 6.62) | 2.5e−05 |
| 6394 | 163 | 2.02 (1.69, 2.41) | 5.4e−15 |

**E**

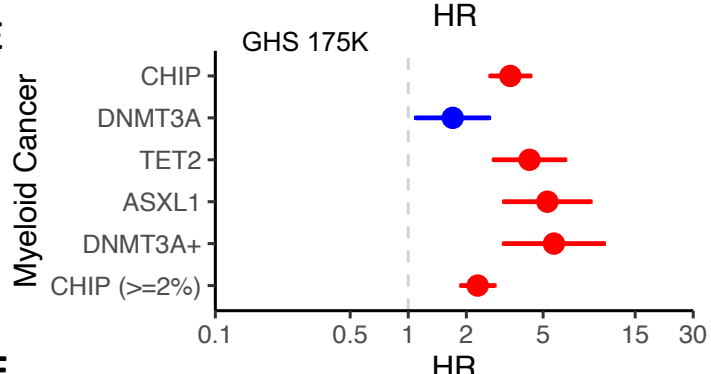


| Total | Event | HR(LCI, UCI) | P-value |
|---|---|---|---|
| 3041 | 83 | 3.38 (2.65, 4.32) | 1.3e−22 |
| 1558 | 21 | 1.7 (1.09, 2.64) | 0.019 |
| 680 | 23 | 4.25 (2.76, 6.55) | 5.2e−11 |
| 346 | 15 | 5.26 (3.12, 8.87) | 4.9e−10 |
| 200 | 11 | 5.69 (3.11, 10.41) | 1.7e−08 |
| 6452 | 121 | 2.29 (1.87, 2.82) | 2.7e−15 |

**F**

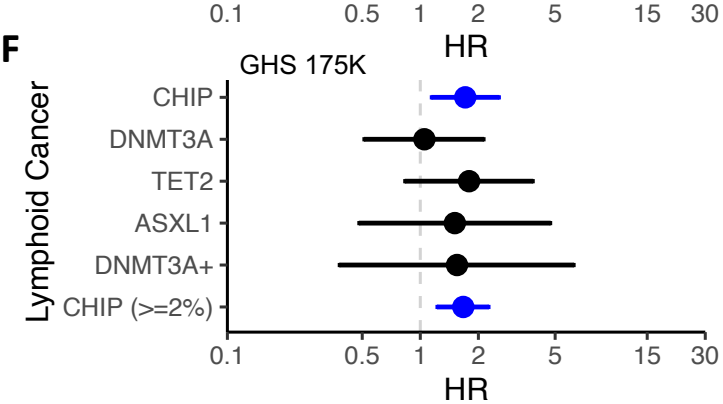


| Total | Event | HR(LCI, UCI) | P-value |
|---|---|---|---|
| 3140 | 28 | 1.71 (1.14, 2.57) | 9.4e−03 |
| 1578 | 8 | 1.05 (0.51, 2.14) | 0.9 |
| 707 | 7 | 1.79 (0.83, 3.85) | 0.13 |
| 356 | 3 | 1.51 (0.48, 4.74) | 0.48 |
| 204 | 2 | 1.55 (0.38, 6.27) | 0.54 |
| 6556 | 53 | 1.67 (1.22, 2.27) | 1.2e−03 |

**Figure S11. Incident risk of blood cancer among CHIP carriers from the UKB and GHS cohorts**
Forest plots and tables featuring hazard ratio estimates from cox-proportional hazard models are shown. CHIP and its most common subtypes are significantly associated with blood (A, D) and myeloid (B, D) cancers, but *DNMT3A*-CHIP is not associated with lymphoid cancers (C, F). Models are adjusted for sex, LDL, HDL, pack years, smoking status, BMI, essential primary hypertension, type 2 diabetes mellitus, and 10 European specific genetic PCs. Hazard ratios (HR) were estimated using cox-proportional hazard modeling, with p-values uncorrected and derived from two-sided Wald tests.

**A**

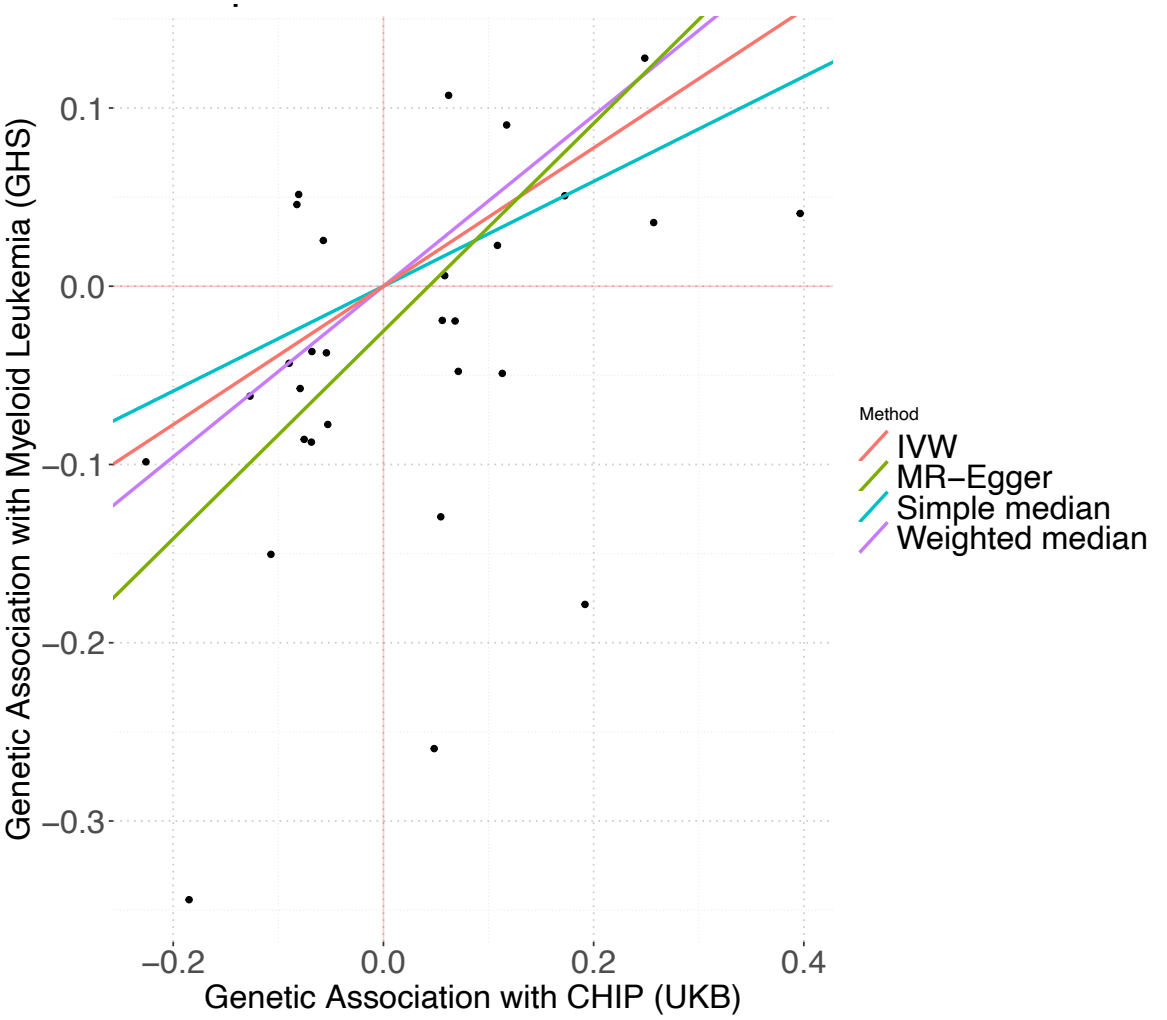


**B**

| **Exposure: CHIP (UKB) \| Outcome: Myeloid Leukemia (GHS)** | | | MR without *TERT* variants | |
|---|---|---|---|---|
| **Method** | **OR (95% CI)** | **P value** | **OR** | **P value** |
| Simple median | 1.34 (0.79-2.29) | 0.28 | 1.34 (0.71-2.55) | 0.37 |
| Weighted median | 1.61 (1.02-2.55) | 0.041 | 1.54 (0.83-2.88) | 0.17 |
| Penalized weighted median | 1.61 (1.02-2.55) | 0.041 | 1.54 (0.83-2.88) | 0.17 |
| IVW | 1.47 (1.05-2.06) | 0.024 | 1.42 (0.91-2.22) | 0.12 |
| Penalized robust IVW | 1.49 (1.15-1.93) | 0.0029 | 1.42 (0.89-2.26) | 0.14 |
| MR-Egger | 1.79 (0.92-3.49) | 0.088 | 1.64 (0.53-5.05) | 0.39 |
| (intercept) | 0.98 (0.91-1.05) | 0.51 | 0.99 (0.89-1.09) | 0.79 |
| Penalized robust MR-Egger | 1.74 (1.17-2.57) | 0.0059 | 1.48 (0.51-4.31) | 0.47 |
| (intercept) | 0.98 (0.92-1.04) | 0.51 | 1.00 (0.90-1.10) | 0.94 |

**Figure S12: MR analysis support causal association between CHIP and Myeloid Leukemia. A.** Plot showing estimated associations via four mendelian randomization (MR) methods between CHIP and Myeloid Leukemia. Each point represents one of 29 instrument variables (i.e. conditionally independent SNPs) that were identified in the UKB cohort as associated with CHIP. The x-axis shows the effect estimate (beta) of the SNP on CHIP in UKB, and the y-axis shows the effect estimate (beta) of the SNP on Myeloid Leukemia in GHS. The slope of each regression line represents the effect size estimated by respective methods. **B.** Statistical results are shown from seven MR methods with differing sensitivities to outliers and/or violations of the MR assumptions. The estimated intercept values are shown for the two MR-Egger-based methods that estimate these terms (yellow rows). The majority of methods support a causal association between CHIP and Myeloid Leukemia, although the signal is no longer significant without the inclusion of *TERT* variants as instrument variables (B, grey text).

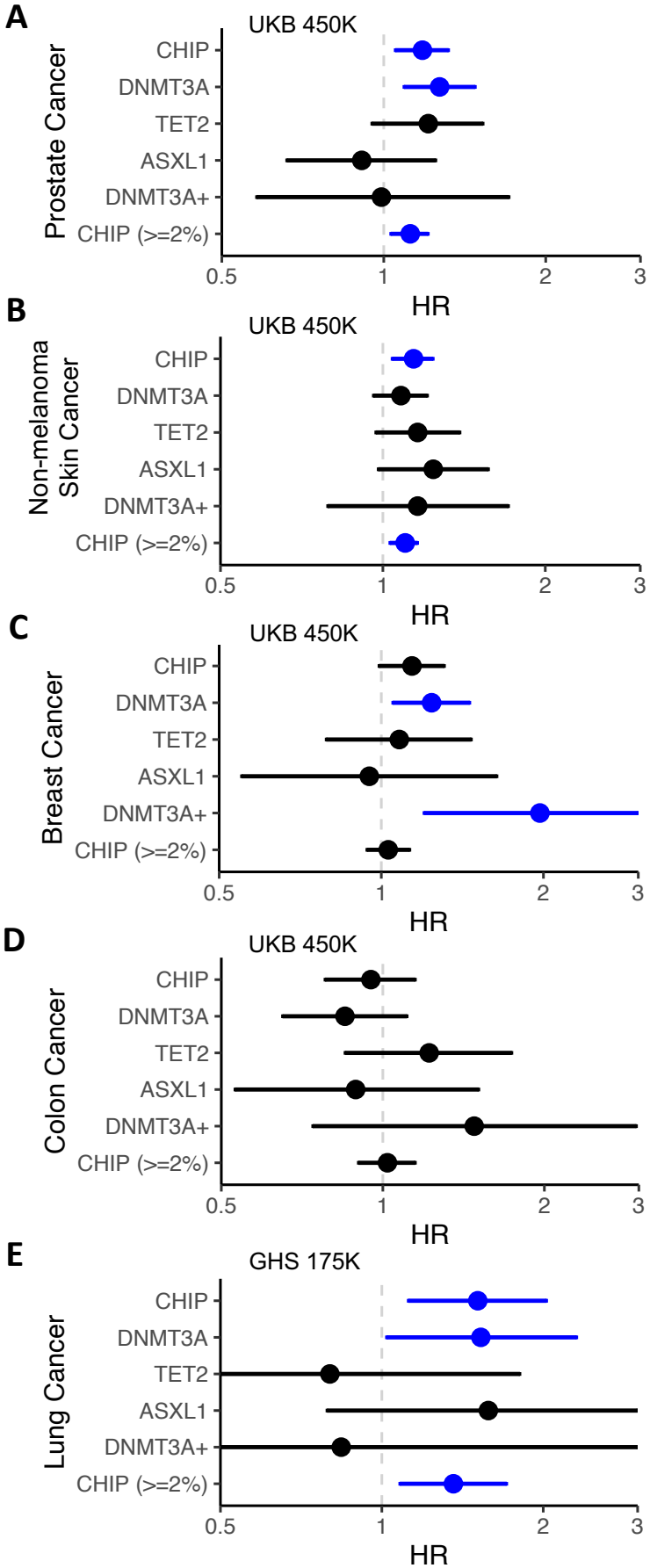


| | Total | Event | HR(LCI, UCI) | P-value |
|---|---|---|---|---|
| CHIP | 4189 | 310 | 1.18 (1.05, 1.32) | 5.3e−03 |
| DNMT3A | 2162 | 172 | 1.27 (1.09, 1.48) | 2.0e−03 |
| TET2 | 894 | 69 | 1.21 (0.95, 1.53) | 0.12 |
| ASXL1 | 656 | 39 | 0.91 (0.66, 1.25) | 0.56 |
| DNMT3A+ | 186 | 13 | 0.99 (0.58, 1.71) | 0.98 |
| CHIP (>=2%) | 9851 | 690 | 1.12 (1.03, 1.21) | 5.3e−03 |

| | Total | Event | HR(LCI, UCI) | P-value |
|---|---|---|---|---|
| CHIP | 8701 | 538 | 1.14 (1.04, 1.24) | 4.7e−03 |
| DNMT3A | 5003 | 286 | 1.08 (0.96, 1.21) | 0.21 |
| TET2 | 1849 | 124 | 1.16 (0.97, 1.39) | 0.11 |
| ASXL1 | 992 | 71 | 1.24 (0.98, 1.57) | 0.079 |
| DNMT3A+ | 434 | 29 | 1.16 (0.79, 1.71) | 0.45 |
| CHIP (>=2%) | 20718 | 1239 | 1.1 (1.03, 1.16) | 1.9e−03 |

| | Total | Event | HR(LCI, UCI) | P-value |
|---|---|---|---|---|
| CHIP | 4521 | 207 | 1.14 (0.99, 1.31) | 0.062 |
| DNMT3A | 2875 | 142 | 1.24 (1.05, 1.46) | 0.013 |
| TET2 | 940 | 41 | 1.08 (0.79, 1.47) | 0.62 |
| ASXL1 | 325 | 13 | 0.95 (0.55, 1.64) | 0.85 |
| DNMT3A+ | 197 | 16 | 1.97 (1.2, 3.21) | 6.9e−03 |
| CHIP (>=2%) | 11034 | 457 | 1.03 (0.94, 1.13) | 0.53 |

| | Total | Event | HR(LCI, UCI) | P-value |
|---|---|---|---|---|
| CHIP | 8891 | 111 | 0.95 (0.78, 1.15) | 0.59 |
| DNMT3A | 5099 | 55 | 0.85 (0.65, 1.11) | 0.24 |
| TET2 | 1889 | 31 | 1.22 (0.85, 1.74) | 0.29 |
| ASXL1 | 1019 | 14 | 0.89 (0.53, 1.51) | 0.68 |
| DNMT3A+ | 445 | 9 | 1.48 (0.74, 2.97) | 0.26 |
| CHIP (>=2%) | 21142 | 275 | 1.02 (0.9, 1.15) | 0.81 |

| | Total | Event | HR(LCI, UCI) | P-value |
|---|---|---|---|---|
| CHIP | 3176 | 51 | 1.51 (1.12, 2.03) | 6.5e−03 |
| DNMT3A | 1592 | 25 | 1.53 (1.02, 2.31) | 0.042 |
| TET2 | 714 | 6 | 0.8 (0.36, 1.81) | 0.6 |
| ASXL1 | 359 | 8 | 1.58 (0.79, 3.2) | 0.2 |
| DNMT3A+ | 208 | 2 | 0.84 (0.21, 3.38) | 0.81 |
| CHIP (>=2%) | 6612 | 91 | 1.36 (1.08, 1.71) | 8.7e−03 |

**Figure S13: Incident risk of solid cancers among CHIP carriers. A-E.** Forest plots and tables featuring hazard ratio estimates from cox-proportional hazard models are shown. CHIP and its most common subtypes are significantly associated with prostate cancer **(A)** and non-melanoma skin cancer **(B)** but not with colon cancer **(D)** in UKB. *DNMT3A*-CHIP is modestly associated (P = 0.013) with breast cancer in UKB, while individuals with a *DNMT3A*-CHIP mutation and at least one additional CHIP mutation (i.e. DNMT3A+) are at a significantly elevated risk of breast cancer **(C)** (OR = 1.97, P = 6.9 x $10^{-3}$). CHIP carriers are at a significantly increased risk of getting lung cancer in GHS **(E)**, which replicated our findings in UKB. Here, results are depicted from analyses in which we removed samples that had a diagnosis of malignant cancer prior to sequencing collection. Models are adjusted for sex, LDL, HDL, pack years, smoking status, BMI, essential primary hypertension, type 2 diabetes mellitus, and 10 European specific genetic PCs. Hazard ratios (HR) were estimated using cox-proportional hazard modeling, with p-values uncorrected and derived from two-sided Wald tests.

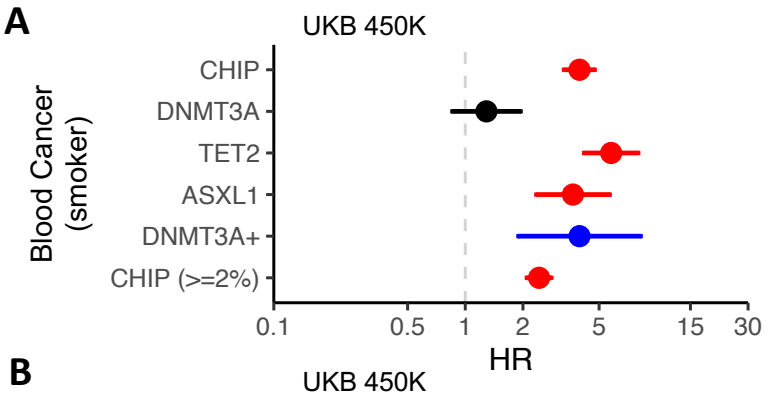


| Total | Event | HR(LCI, UCI) | P-value |
|---|---|---|---|
| 3266 | 205 | 3.95 (3.25, 4.78) | 2.8e−44 |
| 1794 | 48 | 1.29 (0.85, 1.96) | 0.23 |
| 625 | 57 | 5.78 (4.14, 8.07) | 8.4e−25 |
| 518 | 39 | 3.65 (2.33, 5.73) | 1.6e−08 |
| 151 | 32 | 3.95 (1.88, 8.31) | 3.0e−04 |
| 7572 | 307 | 2.43 (2.08, 2.84) | 1.6e−29 |

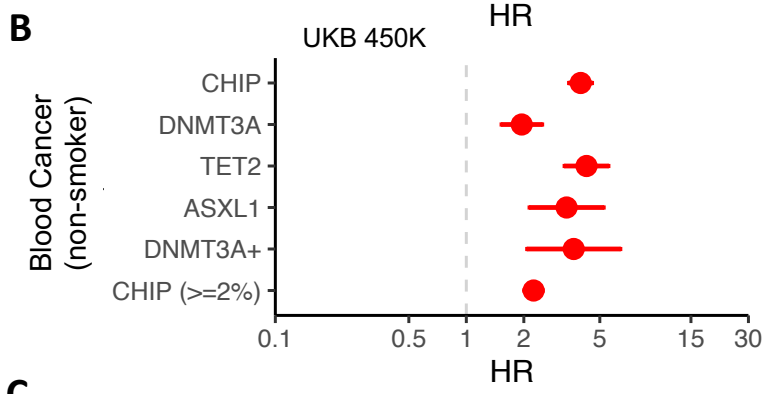


| Total | Event | HR(LCI, UCI) | P-value |
|---|---|---|---|
| 5560 | 315 | 3.97 (3.43, 4.58) | 1.1e−77 |
| 3297 | 100 | 1.95 (1.52, 2.51) | 2.3e−07 |
| 1255 | 87 | 4.26 (3.25, 5.58) | 1.1e−25 |
| 497 | 37 | 3.35 (2.13, 5.27) | 1.9e−07 |
| 288 | 49 | 3.65 (2.07, 6.44) | 7.8e−06 |
| 13497 | 469 | 2.25 (2, 2.53) | 1.9e−41 |

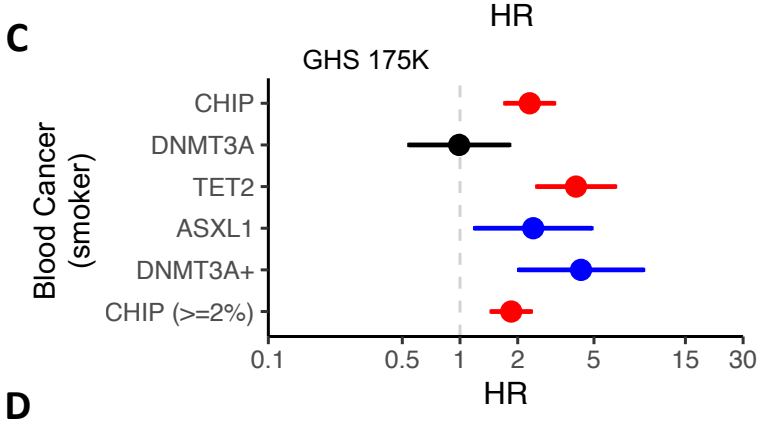


| Total | Event | HR(LCI, UCI) | P-value |
|---|---|---|---|
| 1368 | 52 | 2.31 (1.71, 3.12) | 5.0e−08 |
| 689 | 11 | 0.99 (0.54, 1.82) | 0.98 |
| 281 | 19 | 4.03 (2.51, 6.49) | 9.4e−09 |
| 200 | 8 | 2.41 (1.19, 4.89) | 0.015 |
| 87 | 7 | 4.28 (2.02, 9.09) | 1.5e−04 |
| 2888 | 85 | 1.85 (1.45, 2.36) | 6.1e−07 |

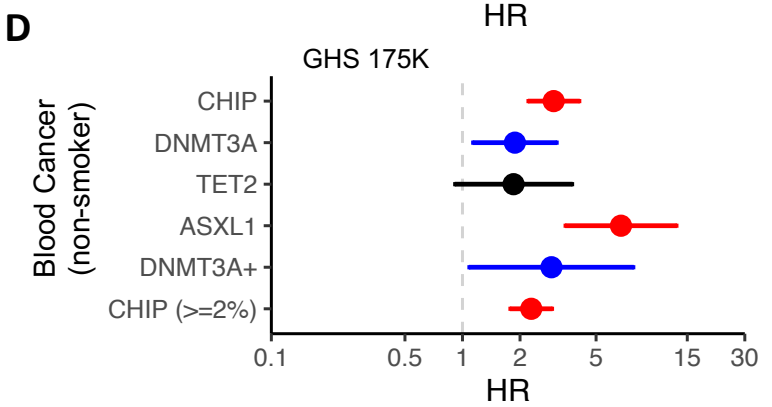


| Total | Event | HR(LCI, UCI) | P-value |
|---|---|---|---|
| 1635 | 49 | 3 (2.2, 4.11) | 6.3e−12 |
| 852 | 16 | 1.88 (1.13, 3.13) | 0.015 |
| 392 | 8 | 1.85 (0.91, 3.77) | 0.092 |
| 143 | 9 | 6.75 (3.44, 13.25) | 2.7e−08 |
| 108 | 4 | 2.92 (1.08, 7.88) | 0.034 |
| 3506 | 78 | 2.29 (1.77, 2.96) | 2.4e−10 |

**Figure S14: Incident risk of blood cancer among CHIP carriers from the UKB and GHS cohorts. A-D.** Forest plots and tables featuring hazard ratio estimates from cox-proportional hazard models are shown. CHIP and its most common subtypes are significantly associated with blood cancer in both smokers and non-smokers across UKB **(A-B)** and GHS **(C-D).** Here, results are depicted from analyses in which we removed samples that had a diagnosis of malignant cancer prior to DNA collection. Models are adjusted for sex, LDL, HDL, pack years, smoking status, BMI, essential primary hypertension, type 2 diabetes mellitus, and 10 European specific genetic PCs. Hazard ratios (HR) were estimated using cox-proportional hazard modeling, with p-values uncorrected and derived from two-sided Wald tests.

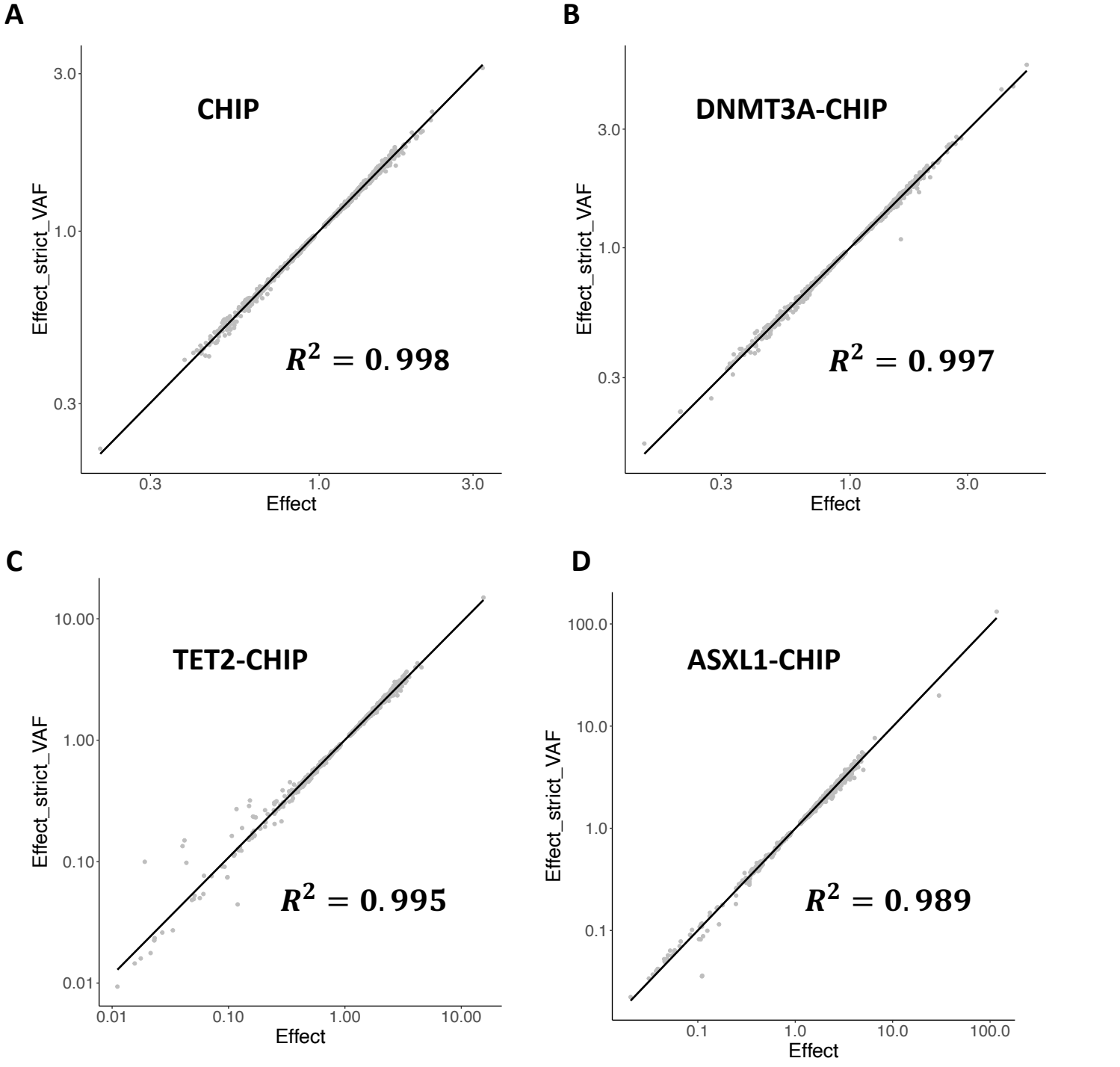


**Figure S15: Effect estimate consistency from sensitivity analyses limiting CHIP callset to variants with VAF < 0.35** Comparison of effect size estimates from our main genetic association results and results performed using a callset that defines carriers after excluding somatic variants from our callset that have VAF >= 0.35. This sensitivity analysis includes variants with alternative allele frequency > 0.001. A-D represent comparisons for CHIP, DNMT3A-CHIP, TET2-CHIP, and ASXL1-CHIP, respectively, and effect estimates are highly consistent in all cases ($R^2$>0.989). See Supplementary Note 11 for additional details.

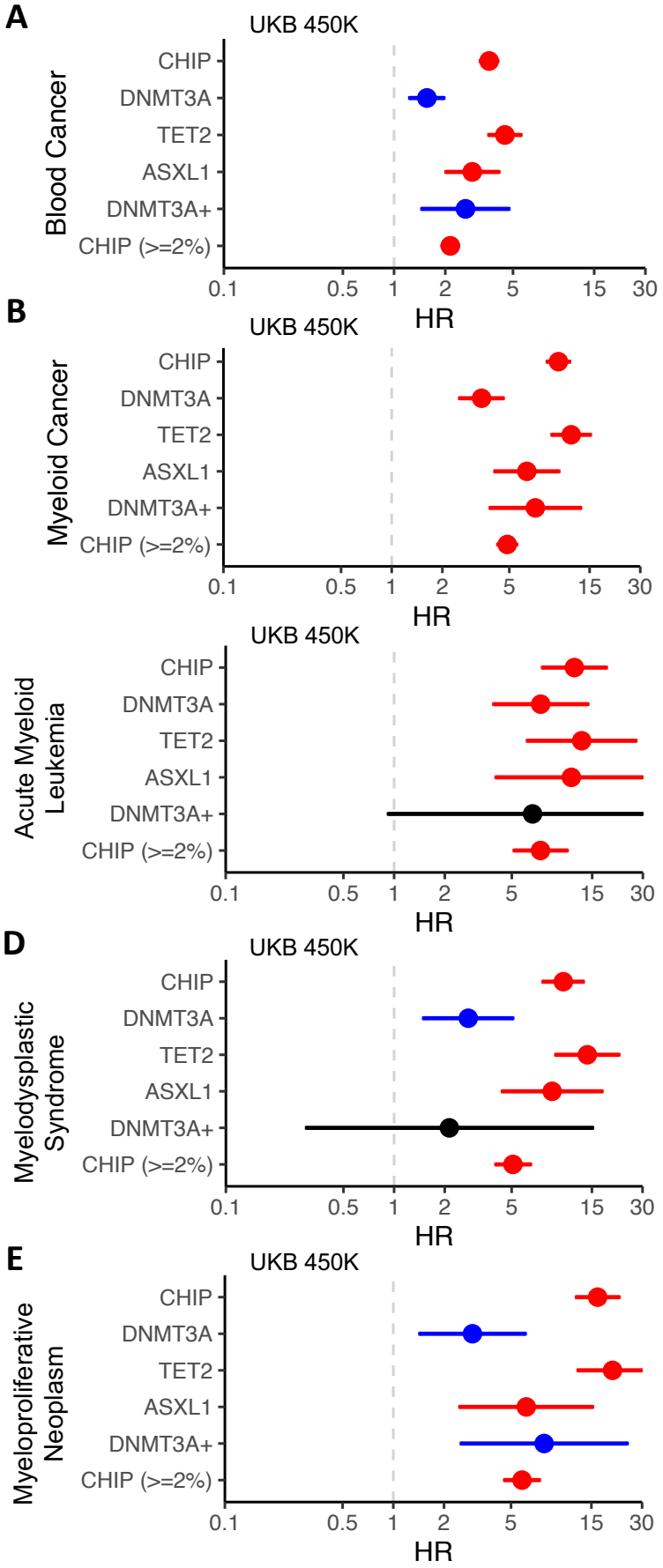


| Total | Event | HR(LCI, UCI) | P-value |
|---|---|---|---|
| 8054 | 441 | 3.62 (3.2, 4.09) | 2.8e−93 |
| 4675 | 120 | 1.56 (1.23, 1.97) | 2.1e−04 |
| 1724 | 123 | 4.48 (3.59, 5.59) | 4.7e−40 |
| 885 | 56 | 2.88 (2.01, 4.15) | 1.1e−08 |
| 357 | 58 | 2.63 (1.45, 4.75) | 1.4e−03 |
| 20346 | 707 | 2.14 (1.94, 2.36) | 1.7e−53 |

| Total | Event | HR(LCI, UCI) | P-value |
|---|---|---|---|
| 8034 | 324 | 9.79 (8.36, 11.46) | 3.5e−176 |
| 4670 | 73 | 3.42 (2.52, 4.62) | 1.7e−15 |
| 1721 | 86 | 11.66 (8.92, 15.24) | 2.3e−72 |
| 884 | 44 | 6.35 (4.08, 9.89) | 2.8e−16 |
| 357 | 37 | 7.14 (3.83, 13.32) | 6.5e−10 |
| 20317 | 444 | 4.86 (4.25, 5.55) | 7.9e−119 |

| Total | Event | HR(LCI, UCI) | P-value |
|---|---|---|---|
| 8099 | 115 | 11.76 (7.57, 18.26) | 5.0e−28 |
| 4679 | 37 | 7.42 (3.89, 14.16) | 1.2e−09 |
| 1730 | 28 | 13 (6.16, 27.43) | 1.7e−11 |
| 888 | 24 | 11.29 (4.01, 31.77) | 4.4e−06 |
| 359 | 27 | 6.64 (0.92, 47.62) | 0.06 |
| 20403 | 169 | 7.4 (5.14, 10.65) | 5.0e−27 |

| Total | Event | HR(LCI, UCI) | P-value |
|---|---|---|---|
| 8089 | 112 | 10.14 (7.65, 13.45) | 3.8e−58 |
| 4677 | 19 | 2.76 (1.49, 5.1) | 1.2e−03 |
| 1728 | 32 | 14.08 (9.1, 21.79) | 1.7e−32 |
| 887 | 23 | 8.7 (4.38, 17.3) | 6.7e−10 |
| 359 | 9 | 2.13 (0.3, 15.16) | 0.45 |
| 20390 | 149 | 5.09 (4.01, 6.47) | 8.0e−41 |

| Total | Event | HR(LCI, UCI) | P-value |
|---|---|---|---|
| 8075 | 87 | 16.34 (12.16, 21.96) | 1.3e−76 |
| 4674 | 8 | 2.95 (1.43, 6.06) | 3.3e−03 |
| 1726 | 26 | 20.03 (12.45, 32.24) | 5.0e−35 |
| 886 | 6 | 6.16 (2.47, 15.34) | 9.4e−05 |
| 359 | 3 | 7.86 (2.52, 24.56) | 3.9e−04 |
| 20369 | 107 | 5.81 (4.56, 7.42) | 2.2e−45 |

**Figure S16: Incident risk of liquid cancers among CHIP carriers defined using VAF < 0.35. A-E.** Forest plots and tables featuring hazard ratio estimates from cox-proportional hazard models are shown. Results are from sensitivity analyses in which CHIP carriers are defined after exclusion of variants with VAF >= 0.35. While results are significant and consistent with our main results, the risk effect size estimates are generally reduced across these hematologic neoplasms. The risks estimates that are most moderated are those for carriers of DNMT3A mutations who also have additional CHIP mutations (DNMT3A+), which is directly consistent with the notion that blanket VAF filtering is eliminating individuals with expanded CHIP (e.g. those with expanded DNMT3A who have subsequently acquired additional mutations). As in our main analyses, models are adjusted for sex, LDL, HDL, pack years, smoking status, BMI, essential primary hypertension, type 2 diabetes mellitus, and 10 European specific genetic PCs. See Supplementary Note 11 for additional details. Hazard ratios (HR) were estimated using cox-proportional hazard modeling, with p-values uncorrected and derived from two-sided Wald tests.

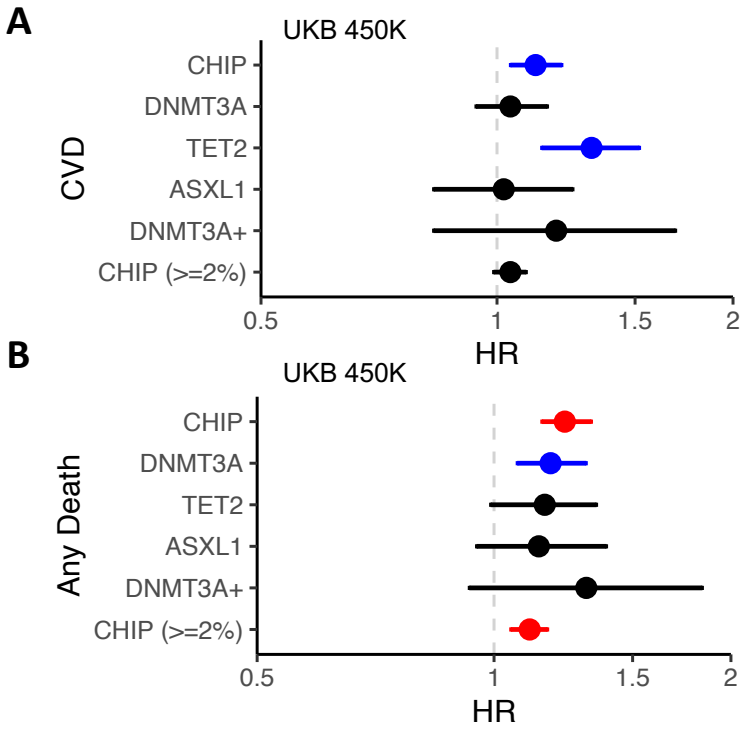


| | Total | Event | HR(LCI, UCI) | P-value |
|---|---|---|---|---|
| CHIP | 7458 | 721 | 1.12 (1.04, 1.21) | 2.1e−03 |
| DNMT3A | 4381 | 362 | 1.04 (0.94, 1.16) | 0.42 |
| TET2 | 1603 | 186 | 1.32 (1.14, 1.52) | 1.7e−04 |
| ASXL1 | 772 | 93 | 1.02 (0.83, 1.25) | 0.86 |
| DNMT3A+ | 294 | 31 | 1.19 (0.83, 1.69) | 0.34 |
| CHIP (>=2%) | 19015 | 1647 | 1.04 (0.99, 1.09) | 0.13 |

| | Total | Event | HR(LCI, UCI) | P-value |
|---|---|---|---|---|
| CHIP | 7601 | 897 | 1.23 (1.15, 1.33) | 2.7e−08 |
| DNMT3A | 4428 | 431 | 1.18 (1.07, 1.31) | 1.2e−03 |
| TET2 | 1645 | 198 | 1.16 (0.99, 1.35) | 0.073 |
| ASXL1 | 796 | 131 | 1.14 (0.95, 1.39) | 0.17 |
| DNMT3A+ | 340 | 79 | 1.31 (0.93, 1.84) | 0.12 |
| CHIP (>=2%) | 19235 | 1849 | 1.11 (1.05, 1.17) | 7.5e−05 |

**Figure S17: Incident risk of CVD and death from any cause among CHIP carriers defined using VAF < 0.35. A-B.** Forest plots and tables featuring hazard ratio estimates from cox-proportional hazard models are shown. Results are from sensitivity analyses in which CHIP carriers are defined after exclusion of variants with VAF >= 0.35. Results are fully consistent with our main results. As in our main analyses, models are adjusted for sex, LDL, HDL, pack years, smoking status, BMI, essential primary hypertension, type 2 diabetes mellitus, and 10 European specific genetic PCs. See Supplementary Note 11 for additional details. Hazard ratios (HR) were estimated using cox-proportional hazard modeling, with p-values uncorrected and derived from two-sided Wald tests.

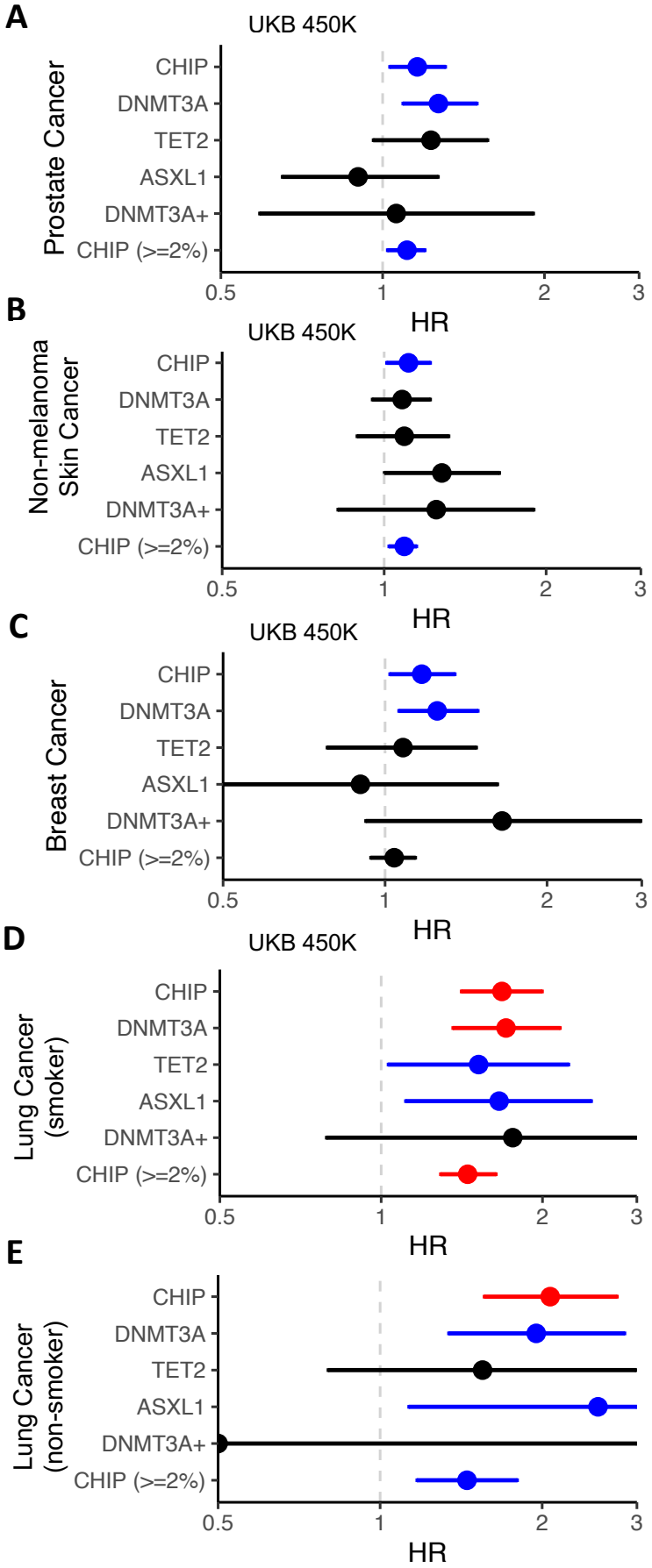


| | Total | Event | HR(LCI, UCI) | P-value |
|---|---|---|---|---|
| CHIP | 3762 | 278 | 1.16 (1.03, 1.31) | 0.014 |
| DNMT3A | 1955 | 156 | 1.27 (1.09, 1.5) | 2.9e−03 |
| TET2 | 819 | 65 | 1.23 (0.96, 1.57) | 0.1 |
| ASXL1 | 572 | 34 | 0.9 (0.65, 1.27) | 0.56 |
| DNMT3A+ | 152 | 11 | 1.06 (0.59, 1.91) | 0.85 |
| CHIP (>=2%) | 9447 | 659 | 1.11 (1.02, 1.2) | 0.012 |

| | Total | Event | HR(LCI, UCI) | P-value |
|---|---|---|---|---|
| CHIP | 7929 | 482 | 1.11 (1.01, 1.22) | 0.031 |
| DNMT3A | 4593 | 263 | 1.08 (0.95, 1.22) | 0.23 |
| TET2 | 1694 | 108 | 1.09 (0.89, 1.32) | 0.4 |
| ASXL1 | 864 | 64 | 1.28 (1, 1.64) | 0.052 |
| DNMT3A+ | 350 | 25 | 1.25 (0.82, 1.9) | 0.3 |
| CHIP (>=2%) | 19998 | 1187 | 1.09 (1.02, 1.15) | 6.7e−03 |

| | Total | Event | HR(LCI, UCI) | P-value |
|---|---|---|---|---|
| CHIP | 4190 | 197 | 1.17 (1.02, 1.35) | 0.03 |
| DNMT3A | 2677 | 134 | 1.25 (1.06, 1.49) | 9.9e−03 |
| TET2 | 869 | 38 | 1.08 (0.78, 1.48) | 0.65 |
| ASXL1 | 289 | 11 | 0.9 (0.5, 1.62) | 0.72 |
| DNMT3A+ | 160 | 11 | 1.65 (0.92, 2.99) | 0.096 |
| CHIP (>=2%) | 10727 | 448 | 1.04 (0.94, 1.14) | 0.43 |

| | Total | Event | HR(LCI, UCI) | P-value |
|---|---|---|---|---|
| CHIP | 2989 | 145 | 1.68 (1.41, 2) | 4.1e−09 |
| DNMT3A | 1650 | 75 | 1.71 (1.36, 2.16) | 5.7e−06 |
| TET2 | 583 | 27 | 1.52 (1.03, 2.24) | 0.036 |
| ASXL1 | 451 | 27 | 1.66 (1.11, 2.47) | 0.013 |
| DNMT3A+ | 130 | 6 | 1.76 (0.79, 3.93) | 0.17 |
| CHIP (>=2%) | 7306 | 308 | 1.45 (1.29, 1.64) | 1.1e−09 |

| | Total | Event | HR(LCI, UCI) | P-value |
|---|---|---|---|---|
| CHIP | 5109 | 51 | 2.07 (1.56, 2.76) | 6.4e−07 |
| DNMT3A | 3028 | 28 | 1.95 (1.34, 2.85) | 5.5e−04 |
| TET2 | 1147 | 9 | 1.55 (0.8, 2.99) | 0.2 |
| ASXL1 | 437 | 6 | 2.54 (1.13, 5.68) | 0.023 |
| DNMT3A+ | 229 | 0 | 0 (0, Inf) | 0.98 |
| CHIP (>=2%) | 13092 | 94 | 1.45 (1.17, 1.8) | 6.8e−04 |

**Figure S18: Incident risk of solid cancers among CHIP carriers defined using VAF < 0.35. A-E.** Forest plots and tables featuring hazard ratio estimates from cox-proportional hazard models are shown. Results are from sensitivity analyses in which CHIP carriers are defined after exclusion of variants with VAF >= 0.35. Results are fully consistent with our main results. As in our main analyses, models are adjusted for sex, LDL, HDL, pack years, smoking status, BMI, essential primary hypertension, type 2 diabetes mellitus, and 10 European specific genetic PCs. See Supplementary Note 11 for additional details. Hazard ratios (HR) were estimated using cox-proportional hazard modeling, with p-values uncorrected and derived from two-sided Wald tests.